

N^* Spectroscopy from Lattice QCD: The Roper Explained

Derek LEINWEBER¹, Waseem KAMLEH¹, Adrian KIRATIDIS¹, Zhan-Wei LIU¹, Selim MAHBUB^{1,2}, Dale ROBERTS^{1,3}, Finn STOKES¹, Anthony W. THOMAS^{1,4} and Jiajun WU¹

¹*Special Research Centre for the Subatomic Structure of Matter (CSSM),
Department of Physics, University of Adelaide, South Australia 5005, Australia*

²*CSIRO, Data61, 15 College Road, Sandy Bay, TAS 7005, Australia*

³*National Computational Infrastructure (NCI),
Australian National University, Australian Capital Territory 0200, Australia*

⁴*ARC Centre of Excellence for Particle Physics at the Terascale (CoEPP),
Department of Physics, University of Adelaide, South Australia 5005, Australia*

E-mail: derek.leinweber@adelaide.edu.au

(Received November 11, 2015)

This brief review focuses on the low-lying even- and odd-parity excitations of the nucleon obtained in recent lattice QCD calculations. Commencing with a survey of the 2014-15 literature we'll see that results for the first even-parity excitation energy can differ by as much as 1 GeV, a rather unsatisfactory situation. Following a brief review of the methods used to isolate excitations of the nucleon in lattice QCD, and drawing on recent advances, we'll see how a consensus on the low-lying spectrum has emerged among many different lattice groups. To provide insight into the nature of these states we'll review the wave functions and electromagnetic form factors that are available for a few of these states. Consistent with the Luscher formalism for extracting phase shifts from finite volume spectra, the Hamiltonian approach to effective field theory in finite volume can provide guidance on the manner in which physical quantities manifest themselves in the finite volume of the lattice. With this insight, we will address the question; Have we seen the Roper in lattice QCD?

KEYWORDS: lattice quantum chromodynamics, baryon spectrum, excited states, wave functions, form factors, finite volume

1. Introduction

In this brief review, we survey recent results for the nucleon spectrum obtained from numerical simulations of lattice QCD. We begin by reviewing the status of the nucleon spectrum as reported by the χ QCD collaboration [1] and the Cyprus group [2] in early 2014. Focusing first on the left-hand plot of Fig. 1, at $m_\pi^2 \sim 0.15 \text{ GeV}^2$ estimates for the mass of the first even parity excitation of the nucleon range from 1.5 GeV by the χ QCD collaboration [1] to 2.5 GeV by the Cyprus group [2].

In comparing the two plots of Fig. 1, aside from the Cyprus group not including the χ QCD collaboration results, the most notable change is a systematic shift of the Cyprus group's results from values $\sim 2.5 \text{ GeV}$ to $\sim 1.8 \text{ GeV}$, a shift much larger than the statistical uncertainties. Cyprus results in the left-hand plot are from version 1 of the arXiv preprint of Ref. [2] from February 2013 whereas the right-hand plot illustrates the results published in Ref. [2] a year later. These results were subsequently improved in the analysis of Ref. [3] by the Cyprus group. It is these final results that have enabled a consensus to form. In the following we will examine the physics behind the evolution of lattice QCD results towards this consensus. However, we will begin with a brief review of the CSSM and JLab Hadron Spectrum Collaboration (HSC) results.

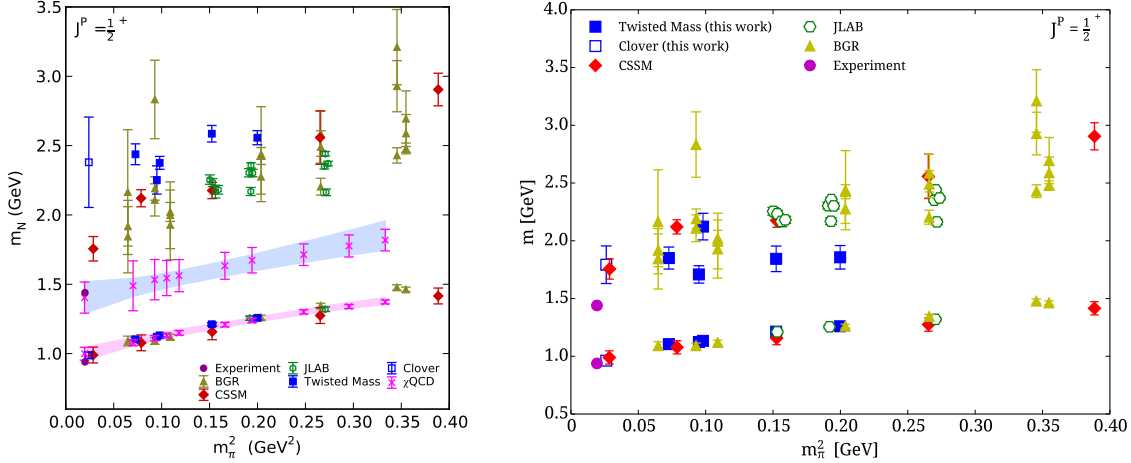


Fig. 1. The low-lying positive-parity spectrum of the nucleon observed in lattice QCD calculations circa January to March 2014. Figures are reproduced from the χ QCD collaboration [1] (left) and the Cyprus group [2] (right). Results from the Berlin-Graz-Regensburg (BGR) collaboration [4], Centre for the Subatomic Structure of Matter (CSSM) [5], JLab Hadron Spectrum Collaboration (JLAB) [6], χ QCD collaboration [1] and Cyprus group (labelled Twisted Mass and Clover) [2] are presented.

2. CSSM and JLab HSC results

In the CSSM approach, a basis of nucleon interpolating fields is created from the three local nucleon interpolating fields with various levels of gauge invariant Gaussian smearing [7] applied to the spatial dimensions of the quark sources and sinks. The superpositions of excited states are dependent on the level of smearing applied [5], such that linear combinations of the smeared sources are constructed to isolate the states of the spectrum through the generalised eigenvalue problem. The outcome of the calculation is a superposition of Gaussians of various widths. Indeed the pattern of the superposition strengths contained in the eigenvectors is precisely that required to create nodes in the excited state wave functions [8].

In the JLab HSC approach [6], a basis of interpolating operators with good total angular momentum in the continuum is developed. These are then subduced to the various lattice irreducible representations by creating lattice derivative operators respecting the cubic symmetry of the lattice. They find that the subduced operators retain a memory of their continuum antecedents to a remarkable degree. While their approach resembles that of a single level of smearing in the quark sources and sinks, the extended nature of their operators aids in isolating the eigenstates of the spectrum.

Fig. 2 presents a comparison of CSSM and JLab HSC results made as the HSC results became available. Despite forming the correlation matrix in completely different manners, the qualitative agreement is remarkable. One must remember that the spatial volumes of the simulations are different and therefore the multi-particle scattering thresholds are different. The CSSM results have a volume with side ~ 3 fm whereas the HSC results are from a smaller volume of ~ 2 fm on a side.

Indeed the most notable discrepancy in Fig. 2 is the first even-parity excitation at $m_\pi^2 \simeq 0.27$ GeV^2 observed by the CSSM. However, this is attributed to the volume dependence of the noninteracting P -wave $N\pi$ scattering threshold given by $E_\pi + E_N$ with $E_i = \sqrt{p^2 + m_i^2}$ and the momentum p governed by the lowest nontrivial momentum on the lattice, $p = 2\pi/L$, where L is the length of the longest spatial dimension. The CSSM point lies just below this threshold. The quantitative agreement between all other states is surprising. The agreement at $m_\pi^2 \simeq 0.17$ GeV^2 for the first even-parity excitation is particularly important in the discussion that follows.

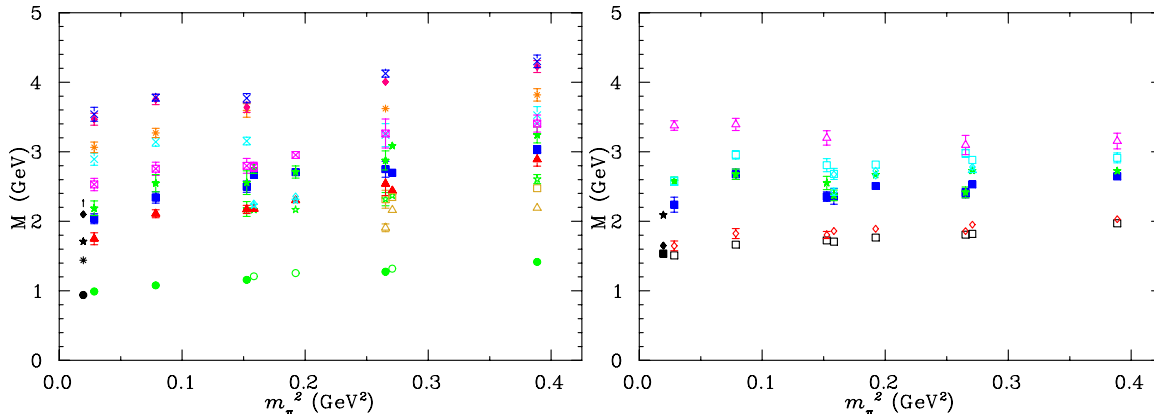


Fig. 2. Comparison of CSSM [5] and JLab HSC [6] results for the low-lying even-parity (left) and odd-parity (right) nucleon spectrum. The three pion masses corresponding to the HSC collaboration are easily identified by the open circles plotted for the ground state nucleon in the left-hand plot.

3. χ QCD Collaboration Results

To better understand the origin of the discrepancy between the χ QCD collaboration results and the CSSM/HSC results depicted in the left-hand plot of Fig. 1, the χ QCD collaboration performed an important controlled experiment [1]. They analysed the gauge fields and quark propagators created by the HSC, thus eliminating all systematic uncertainties other than the final analysis of the baryon correlator. The lightest of the three HSC ensembles were considered where $m_\pi^2 \simeq 0.17 \text{ GeV}^2$. In the usual tradition, they analysed the proton correlation function generated from $\chi_1(x)\bar{\chi}_1(0)$ where $\chi_1(x) = \varepsilon^{abc}(u^\tau a(x) C \gamma_5 d^b(x)) u^c(x)$ is the traditional local nucleon interpolating field. Using their Sequential Empirical Bayesian analysis, they resolved the mass of the first even-parity excitation of the nucleon to be 300 MeV below that obtained by the HSC collaboration [1].

In accounting for this discrepancy, the χ QCD collaboration pointed to the small size of the HSC collaboration's quark-propagator source arguing that they would not be sensitive to the node in the wave function of the first even-parity excitation. Fig. 3 illustrates the node structure observed by the CSSM collaboration. The χ QCD collaboration argued that the basis of interpolators considered by the HSC collaboration was insufficient to span the space, thus producing an erroneously large excitation energy.

However, this is not the case. As illustrated in Figs. 1 and 2, the CSSM result for the first excited state is in excellent agreement with the HSC result at $m_\pi^2 \simeq 0.17 \text{ GeV}^2$. A key feature of the CSSM approach is to consider unusually large fermion source sizes to ensure the correlation matrix basis is sensitive to the node and does indeed effectively span the space of relevant basis states for the low-lying spectrum. This was explored extensively in Ref. [5] where RMS smearing radii from 0.1 to 1.5 fm were investigated, extending well beyond the node at 0.83 fm.

We will return to this issue again after discussing the Athens Model Independent Analysis Scheme employed by the Cyprus collaboration.

4. Athens Model Independent Analysis Scheme

The Athens Model Independent Analysis Scheme (AMIAS) explored by the Cyprus group [3] is a robust and complementary approach to the analysis of hadron correlation functions. Its strength lies in that it does not require human intervention in identifying plateaus in effective mass plots. Indeed it has been key is revising the Cyprus' group's earlier nucleon spectrum results [2] and thus forming a consensus among the Cyprus, JLab and CSSM collaborations on the low-lying excitation spectrum of the nucleon.

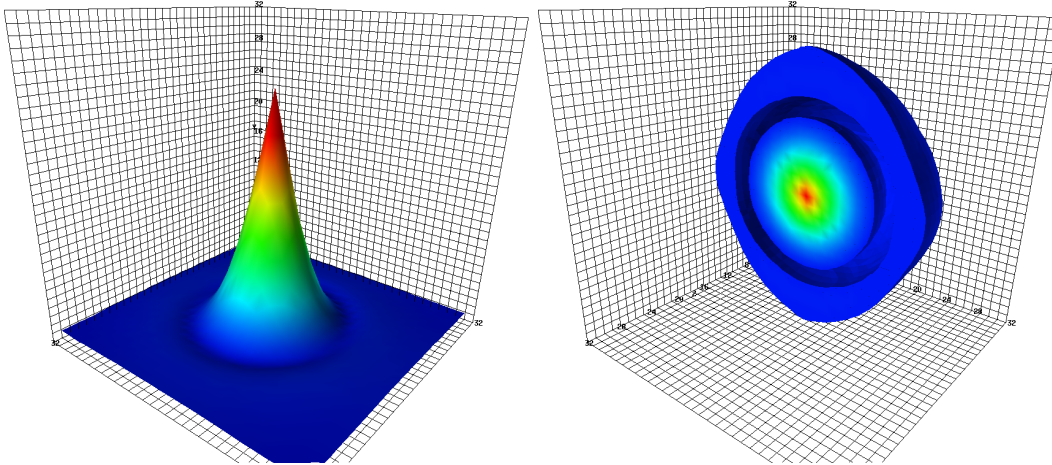


Fig. 3. The d -quark probability distribution in the first even parity excitation of the nucleon about two u quarks fixed at the origin at the centre of the plots [9, 10]. The CSSM calculations are at the lightest of quark masses considered providing $m_\pi = 156$ MeV [11]. The isovolume threshold for rendering the probability distribution in the right-hand plot is 3.0×10^{-5} . The node occurs at 0.83 fm from the centre. The three-dimensional axis grid provides an indication of the positions of the 32^3 lattice sites for the isovolume. The PACS-CS scheme for determining the lattice spacing provides $a = 0.0907(13)$ fm.

The AMIAS method works with the same matrix of correlation functions considered in the standard generalised eigenvalue approach. It exploits the small time separations in the correlation functions where the excited states contribute strongly and statistical errors are small. One considers the standard spectral decomposition of the correlation matrix

$$G_{ij}(t) = \sum_{\alpha=0}^{N_{\text{states}}} A_i^\alpha A_j^{\dagger\alpha} e^{-E_\alpha t}. \quad i, j = 1, \dots, N_{\text{interpolators}}, \quad (1)$$

where E_α is the energy of eigenstate α (increasing with increasing α) and the amplitudes A_i^α and $A_j^{\dagger\alpha}$ indicate the overlap with the j 'th source interpolating and i 'th sink interpolating field with state α .

However, what sets this approach apart from other approaches is that it uses Monte Carlo-based importance sampling to determine the parameters of the spectral decomposition, A_i^α and E_α . Using a parallel-tempering algorithm to avoid local-minima traps [3], values are proposed and selected with the probability $\exp(-\chi^2/2)$, governed by the χ^2 of the fit. Final parameter values and uncertainties are determined by fitting a Gaussian to their probability distributions. The number of states required in the fit, N_{states} , is determined by increasing the number of states until the highest states show no preference in their fit values.

Figure 4 illustrates the key results of Ref. [3]. In the smeared-operator correlation matrix approach, the combination of both large and small smearing extents is critical to obtaining the correct first positive-parity excitation of the nucleon. One cannot get the correct result from the analysis of a single correlator, even when the source is large enough to span the node of the first excitation. There is insufficient information in a single correlation function to correctly reproduce the spectrum observed when analysing all $5 \times 5 = 25$ correlation functions.

This then raises a concern in the Sequential Empirical Bayesian analysis which focuses on a single correlation function. With insufficient information in the single correlator, one becomes concerned about the role of the algorithm in producing a low-lying result for the first positive-parity excitation of the nucleon.

The CSSM collaboration has had a first look at the electromagnetic form factors of the lowest lying even- and odd-parity nucleon excitations [12, 13]. The electric form factors [12] confirm a significantly larger distribution of the quark flavours in these states. Remarkably at heavier quark masses,

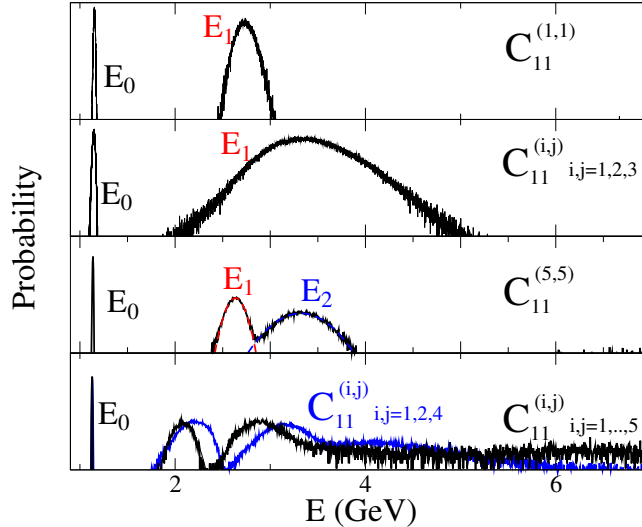


Fig. 4. Reproduced from the Cyprus’ group’s work investigating the Athens Model Independent Analysis Scheme (AMIAS) [3] this plot illustrates the positive parity nucleon spectrum with various subsets of their 5×5 correlation matrix obtained from the $\chi_1(x)\bar{\chi}_1(0)$ correlator with increasing levels of Gaussian smearing applied in the quark sources and sinks. The results in black in the bottom panel of the figure indicate the best results obtained from an analysis of the entire correlation matrix, showing a first excitation at ~ 2.1 GeV relative to a ground state nucleon at ~ 1.2 GeV. The top panel illustrates results obtained from a single correlator with a small amount of smearing. The second panel illustrates results from a subset of the correlation matrix where the smearing of the interpolating fields is small and insensitive to the node in the wave function of the first excitation. Similar to the top panel, the third panel illustrates single correlator results, but this time with a large smeared source considered. The blue curve in the bottom panel omits the third and fifth (largest) of the smeared source/sink correlators.

the first even parity excitations produce magnetic moments similar to the ground state nucleons, consistent with the idea of a $2s$ -state excitation [13]. In the odd parity sector, the lowest lying excitation has magnetic moments consistent with quark model expectations [13].

5. A consensus is established

Having ascertained the necessity of analysing a matrix of correlation functions constructed with a variety of sources sensitive to the node structures of the excited-state wave functions, we are now able to update the results of Fig. 1.

In doing so the CSSM collaboration has updated the statistics of the results published in Refs. [8] and [14] to approximately 29,500 propagators on the PACS-CS configurations [11]. Recall, these lattices have a spatial length $L \simeq 3.0$ fm. The Cyprus group’s results [3] are based on twisted-mass fermion simulations and Wilson-clover simulations from the QCDSF collaboration [15] at the lightest quark mass considered. Their volumes have length $L \simeq 2.8$ fm. Complete details are provided in Ref. [3]. The JLab HSC results [6] are based on anisotropic Wilson-clover lattices with length $L \simeq 2$ fm.

Figure 5 presents results for the ground and first even-parity excitation of the nucleon, and the first three low-lying odd-parity states observed in lattice QCD calculations. In the odd-parity sector, new results from Lang and Verduci [16] are presented alongside new CSSM results [17] demonstrating the robust nature of CSSM analysis methods. Both of these results investigate new interpolating fields for exciting the N^* spectrum.

In the CSSM approach local five-quark operators resembling $N\pi$ states are considered. While the total momentum of the $N\pi$ system is constrained to zero, all possible momenta between the nucleon

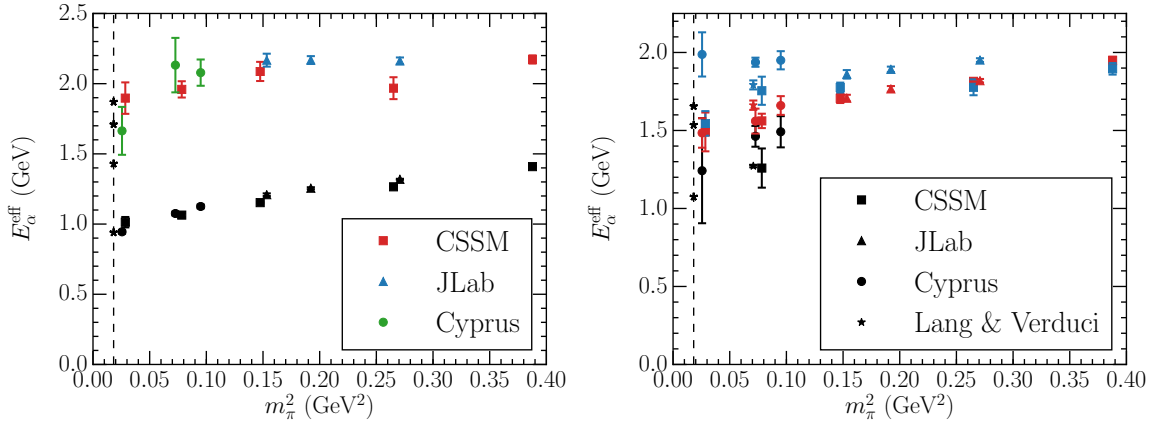


Fig. 5. Current results for the positive-parity (left) and negative-parity (right) nucleon spectrum as reported by the collaborations CSSM [8, 17] and herein, Cyprus [3], JLab [6] and Lang and Verduci [16]. Results for the first two even-parity states of the nucleon are illustrated, while the first three states (identified by the colour of the plot symbols) are presented in the odd-parity channel. Experimental results are illustrated on the vertical dashed line at the physical pion mass. A consensus on the low-lying spectrum has emerged among these lattice groups.

and pion are allowed. In contrast, Lang and Verduci [16] project the momenta of both the nucleon and pion to zero, creating very strong overlap with the lowest lying $N\pi$ scattering state in the finite volume of the lattice.

Both the JLab HSC [6] and CSSM [14] collaborations were able to resolve two low-lying resonant-like states near the $N(1535)$ and $N(1650)$ of nature. They were able to do so without accessing the lowest-lying $N\pi$ scattering state. However, Lang and Verduci found it necessary to include the momentum projected $N\pi$ interpolating field with their analysis techniques [16]. While some have argued that the $N\pi$ scattering state must be observed to get the rest of the spectrum correct, this is not the case [17]. Inclusion of the $N\pi$ scattering state is sufficient [16], but not necessary [17].

6. Have we seen the Roper?

In answering this question, one must have a formalism for connecting the finite-volume spectrum of lattice QCD to the infinite-volume *resonances* of nature. The CSSM collaboration has been investigating Hamiltonian Effective Field Theory (HEFT) [19] to make this connection. Similar to the original idea of Luscher [20, 21], HEFT provides a robust link between the energy levels observed in the finite volume of lattice QCD and the Q^2 dependence of the scattering phase shift. In this way, the CSSM [18] has drawn on experimental data for the scattering phase shift, inelasticity and pole position of the lowest-lying $J^P = 1/2^+$ nucleon resonance, the Roper resonance [22], and used HEFT to predict the positions of the finite-volume energy levels to be observed in lattice QCD simulations in volumes of ~ 3 fm.

The lattice simulation results from the CSSM and Cyprus collaborations employ three-quark operators to excite the spectrum. For three-quark operators, the couplings to two-particle dominated scattering states are volume suppressed by $1/L^3$. As both collaborations consider relatively large lattice volumes with $L \sim 3$ fm, the HEFT states having the largest contribution from the bare basis state are the states more likely to be observed in the lattice QCD simulations. For example, in the ground state nucleon, the bare state is the dominant contribution, providing $\sim 80\%$ of the basis-state contributions.

Figure 6 illustrates the positions of the energies from the HEFT calculation with one bare mass coupled to $N\pi$, $N\sigma$, and $\Delta\pi$ intermediate states [18]. The colour coding of the lines denotes the

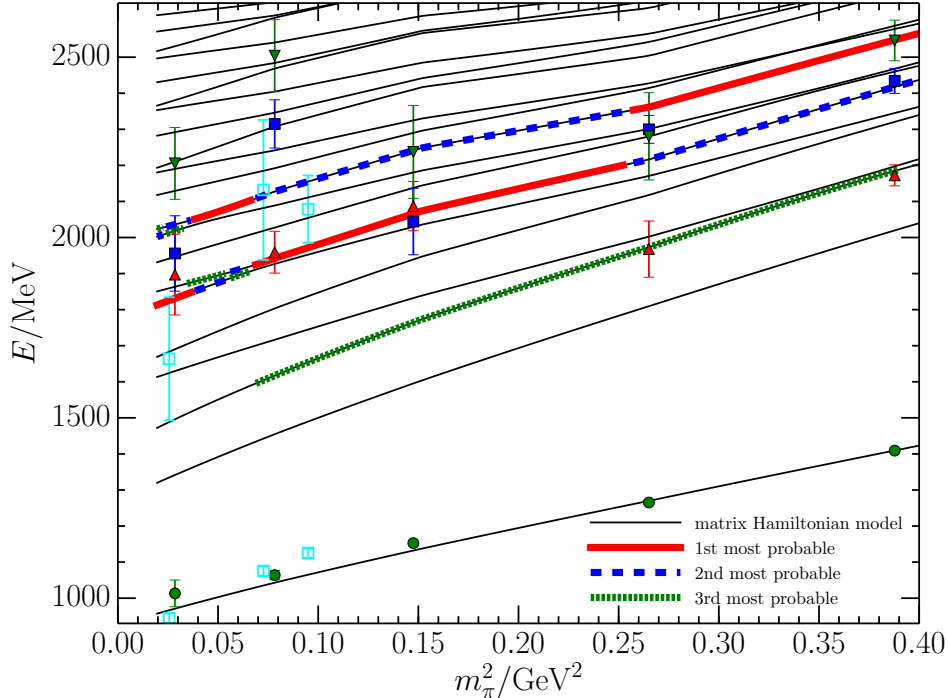


Fig. 6. Finite-volume energy eigenstates for the positive-parity nucleon spectrum from Hamiltonian Effective Field Theory [18] are compared with CSSM and Cyprus collaborations, the latter indicated in cyan. These finite-volume states with $L \sim 3$ fm correspond to a dynamically-generated infinite-volume Roper-resonance pole position in agreement with the particle data tables. States having a significant bare state component – and thus more likely to be excited by three-quark operators – are labelled “most probable” and marked solid red (4 to 5%), dashed blue (3 to 4%) and dotted green ($\sim 1\%$), where the percentage values indicate the typical bare mass contribution to the eigenstate.

excited states having the largest bare-state component and thus the most likely states to be excited in the CSSM and Cyprus simulations. Agreement between HEFT predictions and lattice QCD results is observed as the lattice QCD results tend to sit on the finite volume energy eigenstates dominated by the bare state component. At the lightest quark masses, most of the bare-state strength lies in the first and second most probable states to be seen in the lattice QCD results, having four to five times the bare-state strength of the third most-probable state. This explains why low-lying scattering states are not seen in lattice QCD at light quark masses.

The lower-lying states of the spectrum are dominated by the nearby noninteracting basis states. Just as the low-lying $\Lambda(1405)$ was found to be a $\bar{K}N$ molecular bound state [23–25], there is no low-lying state in the regime of the Roper resonance with a significant bare state component. In order of increasing energy, the excited states are dominated by $N\sigma(p=0)$, $N\pi(p=1)$, $N\sigma(p=0)$ and a mix of $N\pi(p=1)$ and $\Delta\pi(p=0)$ for the fourth excitation. Here, the momenta in parentheses indicate the back-to-back momenta of the meson and baryon in units of $2\pi/L$. Future lattice QCD simulations will aim to excite these scattering states and accurately determine their energies. In this way one can constrain the HEFT from the first principles of QCD and examine the manner in which QCD gives rise to the resonance properties of the Roper excitation.

On the basis of our present analysis we conclude that we have seen at least part of the the Roper in lattice QCD, the part looking most like constituent quark model expectations [10]. The HEFT model describes the Roper resonance of nature as a dynamically generated resonance composed of only a small bare-state component, observed in the region of the finite-volume lattice QCD results.

This research is supported by the National Computational Merit Allocation Scheme and the Australian Research Council through grants DP150103164, DP14010306, DP120104627 and LE120100181.

References

- [1] K.-F. Liu, Y. Chen, M. Gong, R. Sufian, M. Sun, and A. Li, *The Roper Puzzle*, *PoS LATTICE2013* (2014) 507, [arXiv:1403.6847].
- [2] C. Alexandrou, T. Korzec, G. Koutsou, and T. Leontiou, *Nucleon Excited States in $N_f=2$ lattice QCD*, *Phys. Rev.* **D89** (2014), no. 3 034502, [arXiv:1302.4410].
- [3] C. Alexandrou, T. Leontiou, C. N. Papanicolas, and E. Stiliaris, *Novel analysis method for excited states in lattice QCD: The nucleon case*, *Phys. Rev.* **D91** (2015), no. 1 014506, [arXiv:1411.6765].
- [4] **BGR** Collaboration, G. P. Engel, C. B. Lang, D. Mohler, and A. Schäfer, *QCD with Two Light Dynamical Chirally Improved Quarks: Baryons*, *Phys. Rev.* **D87** (2013), no. 7 074504, [arXiv:1301.4318].
- [5] **CSSM Lattice** Collaboration, M. S. Mahbub, W. Kamleh, D. B. Leinweber, P. J. Moran, and A. G. Williams, *Roper Resonance in 2+1 Flavor QCD*, *Phys. Lett.* **B707** (2012) 389–393, [arXiv:1011.5724].
- [6] R. G. Edwards, J. J. Dudek, D. G. Richards, and S. J. Wallace, *Excited state baryon spectroscopy from lattice QCD*, *Phys. Rev.* **D84** (2011) 074508, [arXiv:1104.5152].
- [7] S. Gusken, *A Study of smearing techniques for hadron correlation functions*, *Nucl. Phys. Proc. Suppl.* **17** (1990) 361–364.
- [8] M. S. Mahbub, W. Kamleh, D. B. Leinweber, P. J. Moran, and A. G. Williams, *Structure and Flow of the Nucleon Eigenstates in Lattice QCD*, *Phys. Rev.* **D87** (2013), no. 9 094506, [arXiv:1302.2987].
- [9] D. S. Roberts, W. Kamleh, and D. B. Leinweber, *Wave Function of the Roper from Lattice QCD*, *Phys. Lett.* **B725** (2013) 164–169, [arXiv:1304.0325].
- [10] D. S. Roberts, W. Kamleh, and D. B. Leinweber, *Nucleon Excited State Wave Functions from Lattice QCD*, *Phys. Rev.* **D89** (2014), no. 7 074501, [arXiv:1311.6626].
- [11] **PACS-CS** Collaboration, S. Aoki et al., *2+1 Flavor Lattice QCD toward the Physical Point*, *Phys. Rev. D* **79** (2009) 034503, [arXiv:0807.1661].
- [12] B. J. Owen, W. Kamleh, D. B. Leinweber, M. S. Mahbub, and B. J. Menadue, *Probing the proton and its excitations in full QCD*, *PoS LATTICE2013* (2014) 277, [arXiv:1312.0291].
- [13] B. Owen, W. Kamleh, D. Leinweber, S. Mahbub, and B. Menadue, *Electromagnetic matrix elements for negative parity nucleons*, *PoS LATTICE2014* (2014) 159, [arXiv:1412.4432].
- [14] M. S. Mahbub, W. Kamleh, D. B. Leinweber, P. J. Moran, and A. G. Williams, *Low-lying Odd-parity States of the Nucleon in Lattice QCD*, *Phys. Rev.* **D87** (2013), no. 1 011501, [arXiv:1209.0240].
- [15] G. S. Bali et al., *Nucleon mass and sigma term from lattice QCD with two light fermion flavors*, *Nucl. Phys.* **B866** (2013) 1–25, [arXiv:1206.7034].
- [16] C. B. Lang and V. Verduci, *Scattering in the πN negative parity channel in lattice QCD*, *Phys. Rev.* **D87** (2013), no. 5 054502, [arXiv:1212.5055].
- [17] A. L. Kiratidis, W. Kamleh, D. B. Leinweber, and B. J. Owen, *Lattice baryon spectroscopy with multi-particle interpolators*, *Phys. Rev.* **D91** (2015) 094509, [arXiv:1501.0766].
- [18] Z.-W. Liu, W. Kamleh, D. Leinweber, F. Stokes, A. Thomas, and J. Wu In preparation.
- [19] J. M. M. Hall, A. C. P. Hsu, D. B. Leinweber, A. W. Thomas, and R. D. Young, *Finite-volume matrix Hamiltonian model for a $\Delta \rightarrow N\pi$ system*, *Phys. Rev.* **D87** (2013), no. 9 094510, [arXiv:1303.4157].
- [20] M. Luscher, *Volume Dependence of the Energy Spectrum in Massive Quantum Field Theories. 1. Stable Particle States*, *Commun. Math. Phys.* **104** (1986) 177.
- [21] M. Luscher, *Volume Dependence of the Energy Spectrum in Massive Quantum Field Theories. 2. Scattering States*, *Commun. Math. Phys.* **105** (1986) 153–188.
- [22] L. D. Roper, *Evidence for a P-11 Pion-Nucleon Resonance at 556 MeV*, *Phys. Rev. Lett.* **12** (1964) 340–342.
- [23] B. J. Menadue, W. Kamleh, D. B. Leinweber, and M. S. Mahbub, *Isolating the $\Lambda(1405)$ in Lattice QCD*, *Phys. Rev. Lett.* **108** (2012) 112001, [arXiv:1109.6716].
- [24] J. M. M. Hall, W. Kamleh, D. B. Leinweber, B. J. Menadue, B. J. Owen, A. W. Thomas, and R. D. Young, *Lattice QCD Evidence that the $\Lambda(1405)$ Resonance is an Antikaon-Nucleon Molecule*, *Phys. Rev. Lett.* **114** (2015), no. 13 132002, [arXiv:1411.3402].
- [25] J. M. M. Hall, W. Kamleh, D. B. Leinweber, B. J. Menadue, B. J. Owen, A. W. Thomas, and R. D. Young, *On the Structure of the Lambda 1405*, *PoS LATTICE2014* (2014) 094, [arXiv:1411.3781].